Thermal disruption of the inherent structure of simple liquids

Randall A. LaViolette and Frank H. Stillinger

AT&T Bell Laboratories, Murray Hill, New Jersey 07974

Short range order in liquids formally may be viewed as an inherent structure (amorphous particle packings) that has been smeared by thermally induced vibrational distortions. In order to study these distortions, we have employed molecular-dynamics computer simulation, with steepest-descent quenching to potential energy minima, for a model system resembling liquefied noble gases. A typical multidimensional path connecting the liquid configuration to its quench packing is found to be tortuous and characteristic of substantial anharmonicity. In this respect, thermodynamically stable liquids differ qualitatively from crystals and low-temperature amorphous solids. On the basis of evidence from quench path geometry, and by observing how particle pairs redistribute as a result of the quench, an hierarchical domain clustering picture emerges to characterize vibrational anharmonicity in liquids.

I. INTRODUCTION

Statistical-mechanical descriptions of the structure and dynamics of the thermodynamic phase of a substance usually involve, as a strategy, the exclusion from further consideration of all but the most important configurations. For example, in a crystalline solid at low temperatures, one usually selects out of all the configurations which the solid might assume only those involving displacements of the zero-temperature crystal which are consistent with the harmonic approximation to the potential energy. The selection of the important configurations in other condensed phases is both complicated and special to each phase. In order to unify this selection process, a phase-independent and formally exact procedure has been devised which separates configurations into two contributions.[1] One contribution, the "inherent structure" of the phase, consists of the mechanically stable packings which each correspond to a minimum on the potential energy hypersurface. The remainder amounts to the thermal fluctuations about these packings. This separation procedure provides a comprehensive conceptual framework in which to identify, e.g., the important structural differences between different phases.[2]

The studies of liquids and solids which have exploited this classification procedure have focused on the details of the inherent structure of the respective phases.[1-6] In this study we instead stress the details of the thermal fluctuations in a simple liquid in order to understand more fully the connection between the directly measurable equilibrium properties and the inherent structure of the liquid. The fluctuations in a liquid are not easily described by simple analytic means, and so we employ molecular-dynamics computer simulations, which we outline in Sec. II. In Sec. III we examine the complicated shape of the multidimensional path which connects a typical configuration of the liquid with a typical configuration contributing to the inherent structure. In Sec. IV we expose the structural consequences of the fluctuations with a careful comparison of the pair correlation functions of, respectively, the equilibrium liquid and its underlying inherent structure. We complete this study in Sec. V with a

discussion of these results. We conclude this Introduction with a review of the separation procedure.

The identification of the inherent structure of a phase begins with a mapping which connects any configuration $(\mathbf{r}_1...\mathbf{r}_N)$ of the N particles to the stable packing corresponding to a nearby local minimum $(\mathbf{r}_1^q...\mathbf{r}_N^q)$ on the potential energy hypersurface $\Phi(\mathbf{r}_1...\mathbf{r}_N)$. The mapping is constructed by solving the steepest descent equations[7]

$$\dot{\mathbf{r}}_i = -\nabla_i \Phi(\mathbf{r}_1...\mathbf{r}_N), \quad i = 1...N. \tag{1}$$

This mapping can be used to identify a basin on Φ which contains all the configurations lying on some steepest-descent trajectory to the given packing. These basins cover the configuration space without gaps or overlap. The number of distinct minima on Φ, and so also of basins, rises exponentially with N. The contributions to the free energy of the packings and of the displacements corresponding to the basin surrounding each of the minima can be made explicit by writing the exact classical canonical partition function Q_{NVT} as[7]

$$Q_{NVT} = \lambda_T^{-3N} \int d\phi^q$$
$$\times \exp\{N[\sigma(\phi^q) - \beta\phi^q - \beta f_v(\beta,\phi^q)]\},$$
$$\beta = 1/k_B T, \quad \lambda_T = (\beta h^2/2\pi m)^{1/2},$$
$$\phi^q = \Phi(\mathbf{r}_1^q...\mathbf{r}_N^q)/N. \tag{2}$$

The distinct potential energy minima are distributed by depth ϕ^q according to $\exp[N\sigma(\phi^q)]$. The basins B_α around each of the minima ϕ_α^q contribute to $f_v(\beta,\phi^q)$, the vibrational free energy per particle, written as

$$\exp[-\beta N f_v(\beta,\phi^q)]$$
$$= \left\langle \int_{B_\alpha} d\mathbf{r}_1...d\mathbf{r}_N \exp\{-\beta[\Phi(\mathbf{r}_1...\mathbf{r}_N) - N\phi^q]\}\right\rangle_{\phi_q}. \tag{3}$$

The brackets $\langle...\rangle_{\phi^q}$ indicate the arithmetic mean of the integrals evaluated in each of the appropriate basins B_α for the given depth ϕ^q. In the thermodynamic limit ($N,V \to \infty$, con-

stant N/V), the integrand in Eq. (2) will become sharply peaked as only the most typical of the basins contribute significantly to Q_{NVT}.[7] The inherent structure of a phase at a specified thermodynamic state thus consists essentially of the packings $(r_1^q...r_N^q)$ which correspond to these typical basins. The equilibrium state consists of vibrational distortions of these packings.

In the low-temperature crystalline phase, thermal fluctuations are usually so small that the inherent structure (which in this case consists only of the zero-temperature crystal) together with only small-amplitude harmonic distortions provide an accurate approximation to the free energy. The appropriate inherent structure together with only harmonic distortions also should be expected to supply an accurate estimate of the free energy of, e.g., glasses, gels, and strongly associated liquids near their respective triple points.[8–10] However, as we indicate below, the thermal fluctuations in simple unassociated liquids correspond to large and anharmonic distortions of the packings for those more loosely bound systems; hence the inherent structure together with only harmonic distortions provide in this case a poor approximation to the short-ranged order and the free energy. In an earlier study of a simple liquid we identified the "single-atom return-distance" distribution as a rough probe of the shape of the basin.[2] As the solid melts, this distribution undergoes a sudden change in functional form, from that characteristic of substantially quadratic basins to one indicative of drastically different shape. In another study of the same model substance, we compared the pair correlation function of the equilibrium liquid with that of its inherent structure. As we indicate in Sec. IV, thermal fluctuations in the liquid conceal important qualitative features of the order in the inherent structure. This contrasts with reports that a similar comparison for a model of liquid water shows no such qualitative obliteration of the order.[10,11] In Secs. III and IV we reveal in greater detail, respectively, the shape of basins and the effect of thermal fluctuations on the pair correlation functions.

II. MOLECULAR DYNAMICS CALCULATIONS

In this study we restrict our attention to a model for Φ appropriate for the heavier rare-gas elements. In our model each pair of atoms interacts according to the "$v5$" potential

$$v(r < a) = A \exp[(r-a)^{-1}](r^{-12} - r^{-5}),$$
$$v(r \geqslant a) = 0,$$
$$a = 2.464\,918\,193, \quad A = 6.767\,441\,448.$$

This pair potential is a finited-ranged version of the venerable Lennard-Jones 12-6 potential.[12] Two advantages accompany the $v5$ model in contrast to the Lennard-Jones case. First, the global minimum of

$$\Phi = \sum_{i<j} v(|\mathbf{r}_i - \mathbf{r}_j|)$$

corresponds to a face-centered-cubic crystal, which is also the observed structure of the rare-gas solids at zero temperature and pressure. Second, numerical studies are facilitated since the interactions are smoothly truncated at finite distance a with $v(r)$ infinitely differentiable at all positive r. The

$v5$ model has been employed and discussed in earlier studies.[2,6,13]

The liquid states were simulated by solving Newton's equations with the Gear–Nordsieck fifth order predictor-corrector algorithm.[14] The time step was adjusted so that the fluctuations and drift of the total energy always remained below one part per million. Constant-volume periodic boundary conditions were applied in all the calculations. The density, $N/V = 1.066\,27$, was chosen so that the pressure would be positive at all temperatures. At this density, the $v5$ solid melts at reduced temperature $T = 2.40$. We used reduced units throughout these calculations, so that the mass and diameter of the $v5$ atom, along with the pair-potential depth, were each set equal to unity. However, we report the length of the dynamical trajectories in units appropriate to argon.

III. BASIN GEOMETRY

We report in detail one steepest-descent trajectory from a liquid configuration to its nearest stable packing in order to display the shape of a portion of a typical basin. To produce such a display, we first selected a configuration from the end of a 5 ps molecular-dynamics trajectory of $N = 1008$ $v5$ atoms interacting in a box of reduced dimension $7.690\,96 \times 7.612\,08 \times 16.147\,66$. This box accommodates an undeformed face-centered-cubic crystal for the N particles (for which $\Phi = -7219.3749$). The temperature of the resulting equilibrated liquid was $T = 5.3$, about twice the melting temperature at this density. The potential energy of the initial configuration was $\Phi = 832.907\,10$. The steepest-descent trajectory was numerically approximated by Euler's algorithm[15]

$$\mathbf{r}_i(t + \Delta t) = \mathbf{r}_i(t) - \Delta t \nabla_i \Phi[\mathbf{r}_1(t)...\mathbf{r}_N(t)]. \quad (4)$$

Initially, $\Delta t = 0.001$. If the potential energy should ever increase, the configuration at time $(t + \Delta t)$ would be rejected, Δt would be diminished, and the algorithm would be reapplied until the condition $\Phi(t + \Delta t) \leqslant \Phi(t)$ had been satisfied. This rejection technique was necessary only at the beginning and at the end of the trajectory. In the latter case, the trajectory was terminated when Δt fell below 10^{-9}. At this point we found the potential energy to have declined to $\Phi = -6474.9435$. The magnitude of the gradient, defined by

$$|\nabla \Phi| = \left[\sum_{i=1}^{N} (\nabla_i \Phi)^2 \right]^{1/2},$$

fell to $|\nabla \Phi| = 2 \times 10^{-7}$. We regard this to be the requisite local minimum of Φ. We required 38 100 evaluations each of the potential energy and of its gradient during the search for this minimum, not including the sections of the trajectory which were repeated with smaller initial Δt to test the reproducibility of the trajectory. Normally, just to locate the potential minimum, we would have employed an algorithm which would have required only about 100 evaluations of the energy and its gradient combined.[16] However, we chose the less efficient Euler algorithm in order to display the basin geometry on a refined scale. We also chose a large system in order to secure a packing which with high probability would
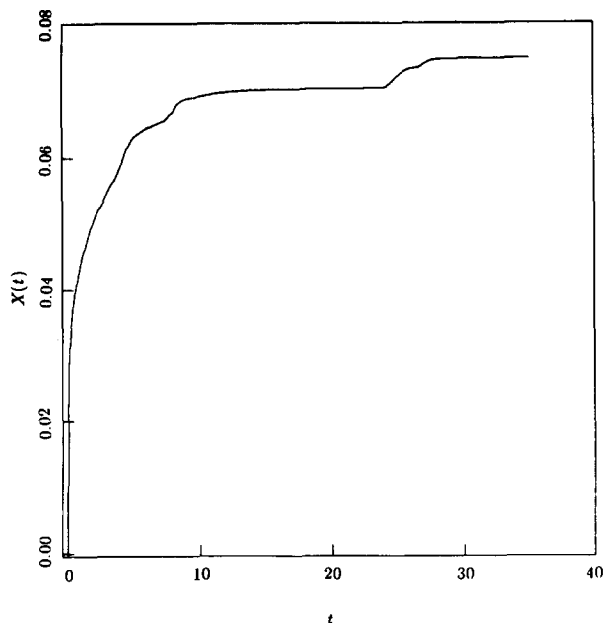
FIG. 1. The path length X as a function of the steepest-descent virtual time t. The sharp bend near $t = 25$ is a reproducible feature.

be closely representative of the inherent structure of the liquid. In fact, the potential energy per particle of the specific minimum found is in excellent accord with the mean potential energy of the inherent structure reported for smaller systems in earlier studies.[2]

At each step of the steepest-descent trajectory we recorded both the potential energy and the magnitude of its gradient. From the latter we produced the length of the path from the initial liquid configuration to the packed structure. The path length $X(t)$ is defined by

$$X(t) = \int_0^t ds \left[\sum_{i=1}^N \dot{\mathbf{r}}_i^2 \right]^{1/2} .$$

According to the steepest-descent equations, $X(t)$ can be written as

$$X(t) = \int_0^t ds |\nabla \Phi| .$$

We write the total path length as $X^q = \lim_{t \to \infty} X(t)$. Figure 1 shows $X(t)$. In order to reveal clearly the anharmonic shape of the basin along the steepest-descent path, we compare both Φ and $|\nabla \Phi|$ to their respective isotropic harmonic oscillator (IHO) approximations along the steepest-descent path. The steepest-descent equations for an isotropic harmonic oscillator,

$$\dot{\mathbf{u}}_i = -\lambda \mathbf{u}_i, \quad i = 1 \ldots N \tag{5}$$

(where $\mathbf{u}_i = \mathbf{r}_i - \mathbf{r}_i^q$), yield

$$|\nabla \Phi|_{IHO} = \lambda |X - X^q| \tag{6}$$

and

$$\Phi_{IHO} = \Phi^q + (\lambda / 2)(X - X^q)^2 . \tag{7}$$

We found $\lambda = 0.725 \pm 0.001$ from a least-squares fit of the first 100 points of the computed $|\nabla \Phi|$ as a function of $X^q - X$. In each of Figs. 2, 3, and 4 we show Φ, Φ_{IHO}, $|\nabla \Phi|$,
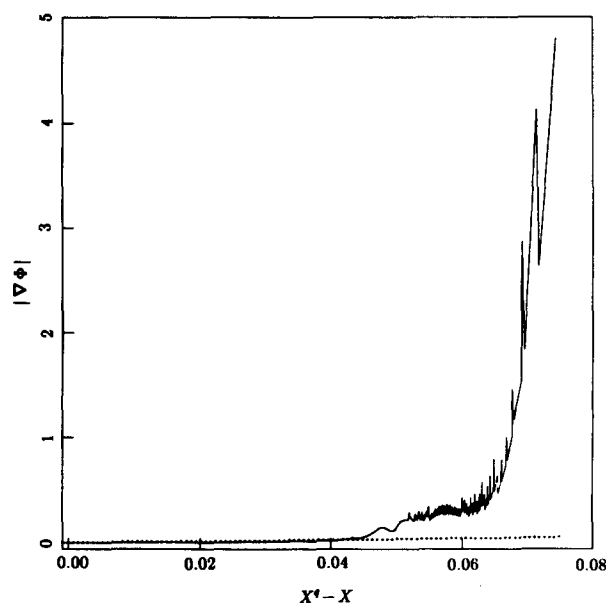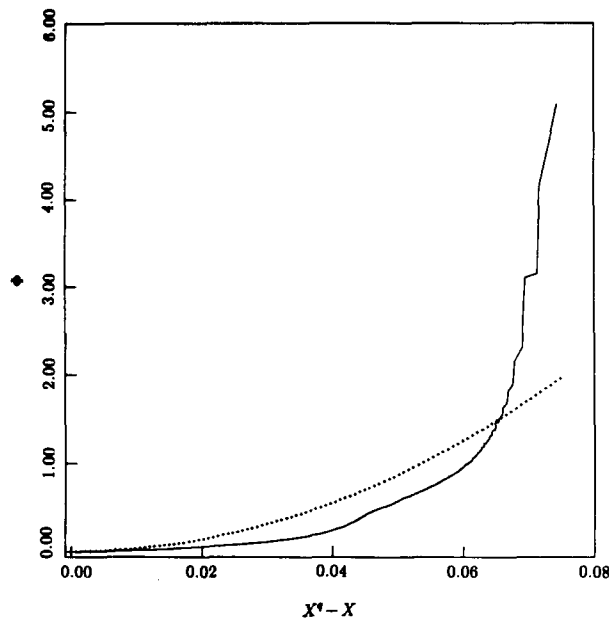

FIG. 2. Panel (a) shows the potential energy as a function of the shifted path length, where both Φ and $X - X^q$ have been divided by $N = 1008$. The solid curve is the computed Φ/N, and the dotted curve is Φ_{IHO}/N [see Eq. (6)]. Panel (b) shows the magnitude of the gradient as a function of the shifted path length, where both have been divided by $N = 1008$. The solid curve is the computed $|\nabla \Phi|/N$, and the dotted curve is $|\nabla \Phi|_{IHO}/N$ [see Eq. (7)]. The plots of Φ/N and $|\nabla \Phi|/N$ each display some algorithm-dependent oscillatory errors in the initial stage of the quench.

and $|\nabla \Phi|_{IHO}$ as a function of the shifted path length $X^q - X$. The nonlinearity of the forces is evident for displacements along the path as small as $X/N = 0.0002$. It should be noted in passing that even for anisotropic quadratic surfaces, $|\nabla \Phi|$ would be a monotonic function of path length, in contradiction with results in Figs. 2(b), 3(b), and 4(b).

We compared the calculated path length to the root-mean-squared "return distance"

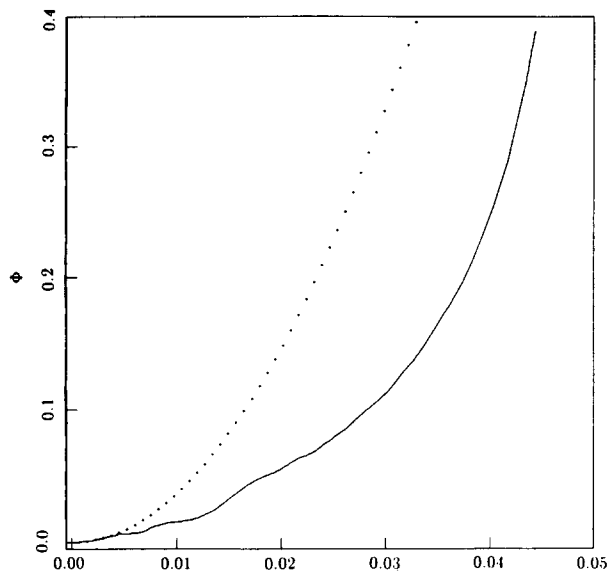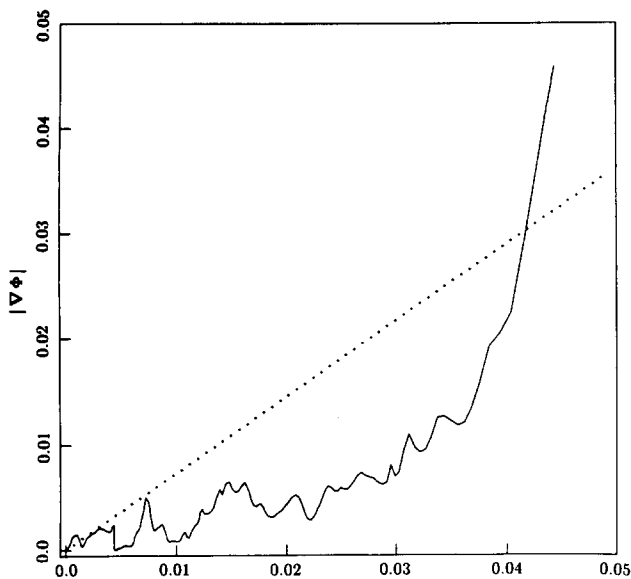$$\delta R = \left[\frac{1}{N} \sum_{i=1}^N (\mathbf{r}_i - \mathbf{r}_i^q)^2 \right]^{1/2}$$

FIG. 3. Expanded view of the neighborhood of the origin for the plots in Fig. 2.

lation function to follow that of the inherent structure, except with shorter and broader peaks, and shallower wells. We would then hope that the equilibrium liquid pair correlation function might be constructed from the convolution of the inherent-structure pair correlation function with a broadening function of the pair distances. Gaussian broadening functions have in fact been employed as filters of low-temperature fluctuations in experimental studies of the structure of crystals and glasses.[17]

On the basis of the presumably typical results discussed in the last section, the basin surrounding any of the minima contributing to the inherent structure of a simple liquid above its melting point is evidently strongly anharmonic along nearly all of each of the relevant steepest-descent paths. However, for temperatures well below the glass transition of the supercooled liquid, the correspondingly short-
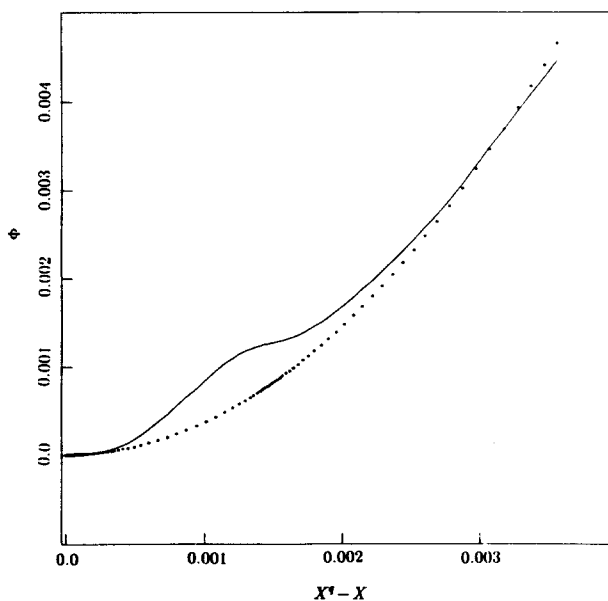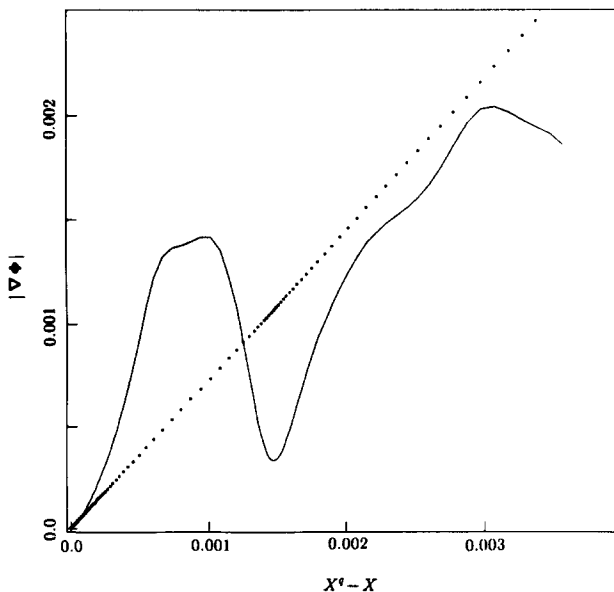

FIG. 4. Further-expanded view of the neighborhood of the origin for the plots in Fig. 2.

between the initial liquid configuration and the packing. In the case of a single isotropic harmonic basin, $\delta R = X^q_{\mathrm{IHO}}/\sqrt{N}$ exactly. Our calculated $X^q/\sqrt{N}$ is actually about $5\delta R$. Although $X^q/\sqrt{N}$ would be greater than or equal to δR for an anisotropic harmonic basin, we believe that this large discrepancy is due mainly to the extreme anharmonicity of the basin compelling the steepest-descent path to follow a meandering route down to the minimum.

IV. PAIR CORRELATIONS

If the thermal fluctuations in a liquid were substantially accounted for by merely harmonic distortions of the underlying stable packings, we would expect the liquid pair corre-

ened return paths and diminished broadening of the pair correlation function of the packings might be adequately approximated by a narrow convolution. To investigate this possibility, we supercooled a liquid (with the same density as above) of $N = 256$ $v5$ atoms interacting in a cubic box of length 6.215 239 4. The box accommodates an undeformed face-centered-cubic crystal. The initial temperature of the equilibrated liquid was $T = 3.00$, about 25% above the melting temperature at this density, and was cooled in steps until the temperature was $T = 0.15$, less than one-third the glass transition temperature at this density.[18] Figure 5 shows the potential energy of both the thermally fluctuating configurations in the glass and the corresponding stable packings generated from steepest descent along the 20 ps molecular-dynamics trajectory. The inherent structure of this glass is probably not representative of that of the equilibrium liquid, since only two packings are included. The temperature-independent inherent structures observed in earlier studies apply strictly only to the equilibrium phases.

The fact that the trajectory crosses a basin boundary after 6.8 ps shows that the configurations sample anharmonic regions of the basins even at this low temperature. The root-mean-square return distance $\langle \delta^2 R \rangle^{1/2}$, averaged for the portions of the trajectory over each of the two basins encountered, provides another measure of anharmonicity. For each basin, $\langle \delta^2 R \rangle^{1/2}$ is, respectively, 0.29 ± 0.02 and 0.26 ± 0.01. Although these distances are only about half of those of the equilibrium liquid, they are half again as great as the maximum root-mean-squared return distance for fluctuations about an undefective crystal near its melting point.[2] We regard these large excursions from the amorphous packings by the atoms in the glassy phase as an indication of the anhar-

FIG. 6. The pair-correlation function of the glass at $T = 0.15$ and its inherent structure. The crosses correspond to $g(r)$, the solid line to $g^q(r)$.

monicity of even those motions remaining at low temperature in the respective basins.

In spite of the indications of anharmonicity, a comparison of the pair correlation functions of, respectively, the glass and its inherent structure (shown in Fig. 6) shows no qualitative change in the structure between the two. The nature of the broadening operation which transforms the inherent-structure pair correlation function $g^q(r^q)$ into the corresponding pair correlation function $g(r)$ of the thermally fluctuating glass is exposed by the joint distribution $N(r, r^q)$ of the pair distances r and r^q. The distribution is constructed by scoring the frequency of the pre- and post-quench pair ($|r_i - r_j|$, $|r_i^q - r_j^q|$) for all pairs of atoms i and j, for each sample. We regard $N(r, r^q)$ as the two-body generalization of the single-atom return-distance distribution.[2] This joint pair distribution was constructed, as were the pair correlation functions, from 100 samples taken from the molecular dynamics trajectory. Figure 7 shows $N(r, r^q)$ from two perspectives, and it is substantially symmetric about the 45° line on this scale.

This picture changes drastically in the case of a thermodynamically stable liquid. In Figs. 8 and 9 we show, respectively, $g^q(r^q)$ and $g(r)$, and $N(r, r^q)$ for the slightly supercooled liquid at $T = 1.94$. The strong, anharmonic thermal fluctuations in the liquid remove much of the short-range order present in the liquid's inherent structure. The qualitative loss of order can be seen immediately by comparing especially the first and second neighbor peaks of, respectively, $g^q(r^q)$ and $g(r)$. The previous 45° symmetry of $N(r, r^q)$ is broken, especially for the nearest-neighbor distances. The asymmetry now present in $N(r, r^q)$ corresponds to the majority of nearest-neighbor distances in the packings increasing upon heating to the liquid. This antisocial tendency is consistent with the well-established dominance of repulsive forces between neighbors in "van der Waals" liquids[19] like $v5$. Note however that $N(r, r^q)$ also shows a small proportion of pairs initially present between first and second peaks of g^q which
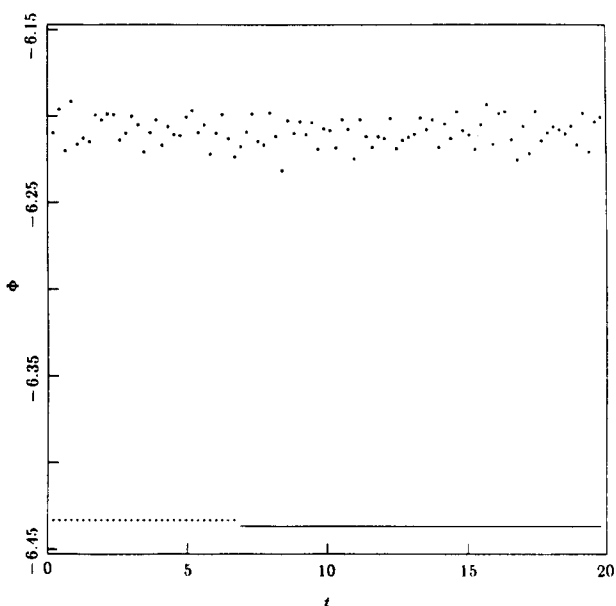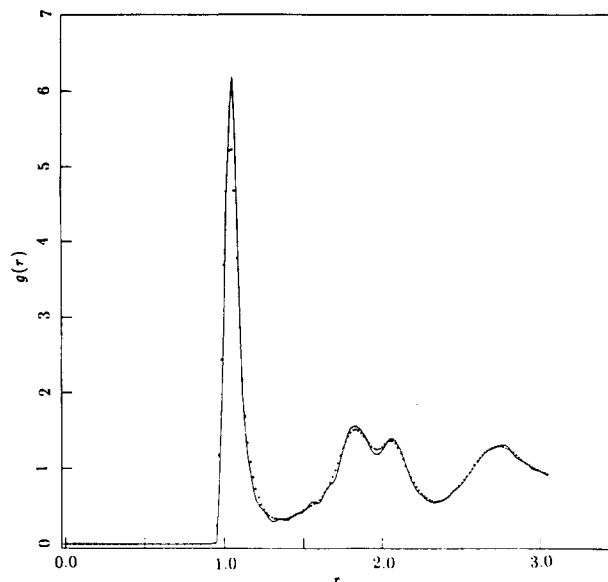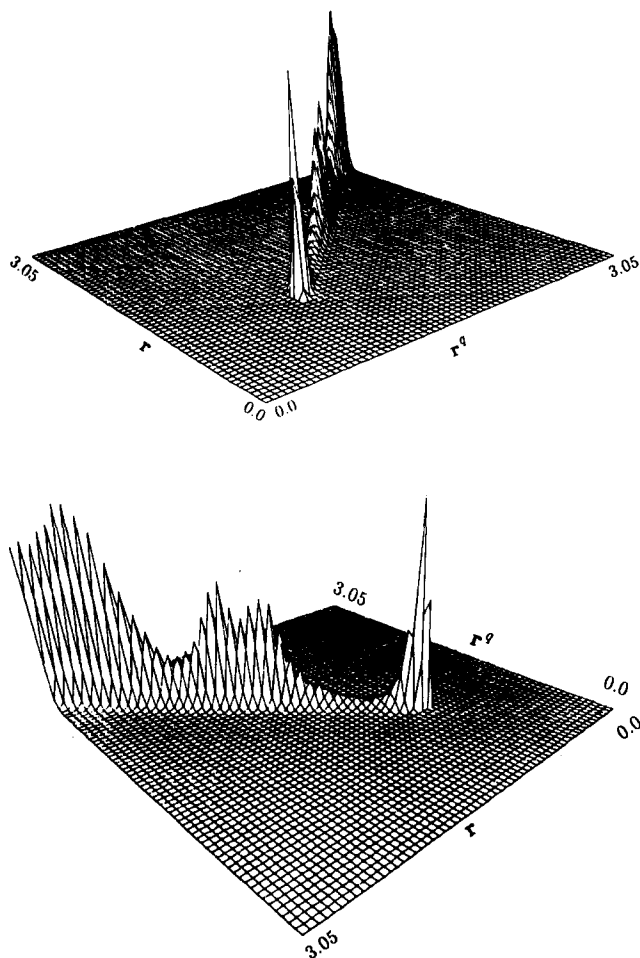

FIG. 5. The potential energy per particle of the instantaneous prequenched (upper cluster of points) and quenched (line and crosses) configurations in the glass at $T = 0.15$, as a function of time in picoseconds. The units of time are appropriate for argon. The "inherent structure" of the glass consists in this case of only two configurations. The crosses correspond to the quenched configuration with a per particle potential energy $\Phi/N = -6.433\,27$, the line to the quenched configuration with $\Phi/N = -6.436\,64$.

FIG. 7. Two views of $N(r,r^q)$ for the glass at $T = 0.15$.

FIG. 9. Two views of $N(r,r^q)$ for the liquid at $T = 1.94$. The perspectives are identical to those in Fig. 7.

have been driven inward to the nearest-neighbor position as a result of the heating process. The complex shape of the $N(r,r^q)$ surface provides some insight into the failure of earlier attempts to map $g^q(r^q)$ into $g(r)$ by a convolution of
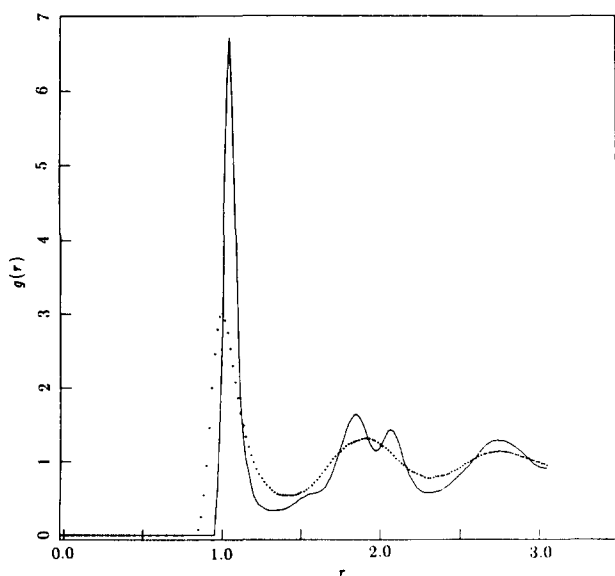

FIG. 8. The pair-correlation function of the liquid at $T = 1.94$ and its inherent structure. The crosses correspond to $g(r)$, the solid line to $g^q(r)$.
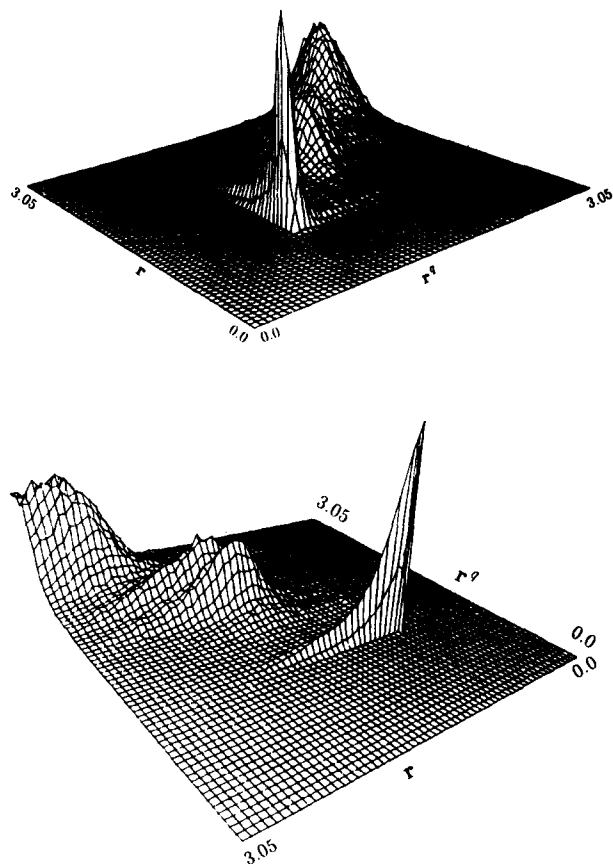
$g^q(r^q)$ with positive real functions.[20] No simple convolution of $g^q(r^q)$ could have reproduced this highly asymmetric distribution of pair distances in the liquid.

V. DISCUSSION

The vibrational distortions of the packings which constitute the inherent structure of either a van der Waals liquid or its glass are characterized by large, asymmetrically distributed displacements. The anharmonicity of the basins surrounding the corresponding potential energy minima stands in contrast to the substantially quadratic shape of the basin containing the crystal minimum. Our depiction of the topography of the basins agrees with and refines our earlier study of the multidimensional geometric aspects of the solid–liquid transition.[2] In both that study and the present one we have shown how these topographical differences are connected to the structural differences between the corresponding packings. In this way we lay the ground for a unified treatment of crystalline, vitreous, and liquid phases.

While we recognize the marked quantitative differences between $g(r)$ and $g^q(r^q)$, both the liquid and its inherent structure possess only short-ranged order. In fact, the inherent structure resembles[4] in many respects the random close-packed structures of hard spheres which Bernal[21] and others employed as models of the short-ranged order in equilibrium liquids. This suggests that we have in the inherent structure not only a formal correspondence to the liquid, but also an

ingredient essential to the structure of the liquid. For the liquid, however, the transformation from the inherent structure to the vibrationally deformed configurations is complicated, as both the typical steepest-descent path and the graph of $N(r, r^q)$ show.

The geometric complexity of the steepest descent path constructed in this study for 1008 particles in three dimensions qualitatively resembles that uncovered earlier (but examined in much less detail) for a different model with 780 particles in two dimensions.[7] In both cases, the paths involved many seemingly irregular changes in slope before the basin bottom was finally encountered. It seems attractive to suppose that an hierarchical sequence of collective processes occurs in both cases. In a typical liquid-state starting configuration, thermal fluctuations will have stirred the particles so that many nearest-neighbor pairs are substantially displaced from the pair-potential minimum and hence subject to strong pair forces. The earliest stage of the steepest descent would quickly relieve these large and localized pair stresses. Subsequently, neighboring pairs would organize to the extent possible into larger stress-free groupings. As virtual time for the steepest descent proceeded, the stress-free clusters or domains would collectively reorient and often merge with neighboring domains. This would eliminate interdomain boundary stresses and result in a larger mean domain size. The characteristic feature is that larger and larger collective units move coherently as the basin bottom is approached. Eventually the domains lock into a structure that is incapable of further stress relief: the local potential minimum has been achieved.

For two-dimensional fluids, the domain structure is easily revealed using Voronoi polygon analysis.[7] The domains consist of crystallites with local sixfold coordination, and these grow in size as thermal fluctuations are removed by the steepest descent mapping. In three dimensions the possible domain crystallite structures and the type of boundary defects are much more numerous, making interpretation of quench paths less straightforward. In any case, typical quenches from the liquid state (with hierarchical domain coarsening) must be qualitatively different from those that start with the crystalline state (with a single macroscopic domain during the entire quench). The drastic change in the return-distance distribution accompanying melting, reported earlier,[2] reflects this distinction.

It should be possible to invent a numerical measure of the liquid-quench hierarchical coarsening. Evidently what is required is a function sensitive to the spatial coherence length of instantaneous particle motions during the course of the steepest descent path. Future quench studies should attempt to incorporate such a running measure of collectivity. The results would also be useful in devising mathematical models for the basin vibrational free energy f_v defined in Eq. (3).

ACKNOWLEDGMENT

[1] F. H. Stillinger and T. A. Weber, Science **225**, 983 (1984).
[2] R. A. LaViolette and F. H. Stillinger, J. Chem. Phys. **83**, 4079 (1985).
[3] F. H. Stillinger and T. A. Weber, J. Chem. Phys. **81**, 5095 (1984).
[4] F. H. Stillinger and T. A. Weber, J. Chem. Phys. **83**, 4767 (1985).
[5] T. A. Weber and F. H. Stillinger, Phys. Rev. B **32**, 5402 (1985).
[6] F. H. Stillinger and R. A. LaViolette, Phys. Rev. B (to be published).
[7] F. H. Stillinger and T. A. Weber, Phys. Rev. A **25**, 978 (1982).
[8] F. H. Stillinger and T. A. Weber, J. Phys. Chem. **87**, 2833 (1983).
[9] T. A. Weber and F. H. Stillinger, J. Chem. Phys. **80**, 438 (1984).
[10] R. A. LaViolette, Ph.D. dissertation, University of California, Berkeley, 1984 (unpublished).
[11] A. Pohorille, R. A. LaViolette, L. R. Pratt, and M. A. Wilson (in preparation).
[12] J. O. Hirschfelder, C. F. Curtis, and R. B. Bird, *Molecular Theory of Gases and Liquids* (Wiley, New York, 1954), p. 1041.
[13] F. H. Stillinger and R. A. LaViolette, J. Chem. Phys. **83**, 6413 (1985).
[14] C. W. Gear, *Numerical Initial-Value Problems in Ordinary Differential Equations* (Prentice–Hall, Englewood Cliffs, NJ, 1971).
[15] G. Dahlquist, A. Bjork, and N. Anderson, *Numerical Methods* (Prentice–Hall, Englewood Cliffs, NJ, 1974), pp. 338 and 441.
[16] L. C. Kaufmann (private communication). This algorithm optimally alternates between steepest-descent and quasi-Newton methods, and for our purposes has proved superior to commercially available minimization routines.
[17] A. C. Wright and A. J. Leadbetter, Phys. Chem. Glasses **17**, 122 (1976).
[18] For a similar system of Lennard-Jones atoms, Fox and Andersen gave $T = 0.5$ for the glass transition temperature. See J. R. Fox and H. C. Andersen, Ann. N.Y. Acad. Sci. **371**, 123 (1981).
[19] D. Chandler, J. D. Weeks, and H. C. Andersen, Science **220**, 787 (1983).
[20] T. A. Weber and F. H. Stillinger, J. Chem. Phys. **81**, 5089 (1984).
[21] J. D. Bernal, Proc. R. Soc. London Ser. A **280**, 299 (1964).